

# CHARACTERIZATION OF THE X-RAY ANGULAR POINTING JITTER IN THE LCLS HARD X-RAY UNDULATOR LINE \*

R. A. Margraf<sup>†1</sup>, J. P. MacArthur, G. Marcus, D. Zhu, T. Sato, Z. Huang<sup>1</sup>  
 SLAC National Accelerator Laboratory, Menlo Park, USA  
<sup>1</sup>also at Stanford University, Stanford, USA

## Abstract

The angular pointing jitter of X-ray pulses produced by an X-ray Free-Electron Laser (XFEL) depends on both intrinsic properties of the SASE (Self-amplified spontaneous emission) process and jitters in beamline variables such as electron orbit. This jitter is of interest to the Cavity-Based XFEL (CBXFEL) project at SLAC, which will lase seven undulators inside an X-ray cavity of four diamond Bragg mirrors. The CBXFEL cavity has a narrow angular bandwidth, thus large angular jitters cause X-rays to leak out of the cavity and degrade cavity efficiency. To understand contributors to angular pointing jitter, we studied the pointing jitter of the Linac Coherent Light Source (LCLS) Hard X-ray Undulator line (HXU). Monochromatic and pink X-rays were characterized at the X-ray Pump Probe (XPP) instrument. We found pulses with high monochromatized pulse energy and small electron beam orbit in the undulator have the lowest angular pointing jitter. We present here our measurement results, discuss why these factors correlate with pointing stability, and propose a strategy for CBXFEL to reduce angular pointing jitter and account for angular pointing jitter in cavity efficiency measurements.

## INTRODUCTION

X-rays produced by a SASE XFEL can exhibit angular pointing jitters, where the far-field X-ray pointing angle differs from the nominal beam axis. As illustrated in Fig. 1, this pointing can be observed as transverse movement of the center of the X-ray spot on a downstream screen. The angular pointing jitter arises from both the intrinsic factor, such as limited transverse coherence and pointing stability of a SASE source [1], and imperfect machine factors, such as the electron beam orbit.

The CBXFEL project [2, 3], will enclose the first seven undulators of the LCLS HXU with a cavity of four diamond (400) Bragg-reflecting mirrors, recirculating X-rays to seed the FEL process for subsequent electron bunches. The FWHM angular bandwidth of a diamond 400 mirror at a 45 degree Bragg angle and 9.831 keV photon energy is 8.8  $\mu$ rad, and the RMS angular divergence of the X-ray beam in CBXFEL is expected to be 1.1 - 1.2  $\mu$ rad [2]. Thus, large angular pointing jitters of several  $\mu$ rad can cause X-rays to exceed the cavity angular acceptance and be out-coupled from the cavity. For smaller angular pointing jitters, such as

those we expect in LCLS, the beam will remain in the cavity, but the X-ray beam will gradually walk off from the optimal overlap with the electron beam axis. Compound refractive lenses (CRLs) can be used to stabilize the X-ray trajectory, causing it to undergo a betatron oscillation about the nominal trajectory. However, in both cases the overlap between the returned X-ray and seeded electron beams is reduced, reducing gain. In this study, we directly measured the X-ray pointing jitter of LCLS to better understand the implications of angular pointing jitter for the CBXFEL project.

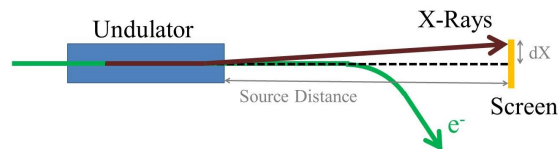


Figure 1: Basic layout of a pointing jitter measurement.

## MEASUREMENT

### Pointing Jitter of Saturated X-ray Beams

We took pointing jitter measurements on three different days, using three different screens in XPP [4] and inside the X-Ray Transport tunnel (XRT). Figure 2 shows a schematic of the HXU beamline with 32 undulators installed. The scintillator screen based cameras in XPP, *Zyla\_0* and *Yag2*, can receive either the full SASE spectrum ("pink beam"), or beam after a double crystal diamond (111) monochromator ("monochromatized beam") [5]. The screen in XRT, *xcs\_yag1*, can receive pink beam simultaneously as monochromatized beam is received in XPP. Our first datasets were taken in November 2020, when only 26 undulators were installed in HXU. On November 9, we measured pink beam on *Yag2*, and on November 13, we measured monochromatized beam on *Yag2*. Additional undulators were installed at the beginning of HXU from December 2020-January 2021, bringing the total undulators to 32. On February 2, 2021, we measured pink beam on *Xcs\_yag1* and monochromatized beam on *Zyla\_0* simultaneously.

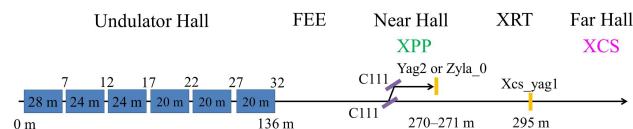


Figure 2: Layout of LCLS HXU Beamline. The monochromator can be removed for XPP screens to receive pink beam.

\* This work was supported by the Department of Energy, Laboratory Directed Research and Development program at SLAC National Accelerator Laboratory, under contract DE-AC02-76SF00515.

<sup>†</sup> rmargraf@stanford.edu

We fit a 2D Gaussian function to the recorded X-ray spots, as shown in Fig. 3, then divided by the source distance to get the angular pointing. Shots with fitted centers falling outside the detector area were discarded. The source distance was defined as the end of the last undulator in the hall that was lasing, because in a SASE FEL, most X-rays are produced in the last gain length. We also recorded the electron beam orbit in HXU using beam position monitors (BPMs), the X-ray pulse energy both for pink (“gas detector energy”) and the the monochromatic slice (“i0”). However, in the November 9th dataset, the i0 detector, located in XPP, saw the full SASE spectrum, not just a monochromatic slice.

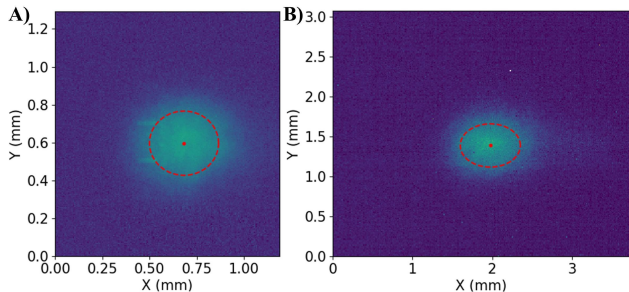


Figure 3: Example of a Gaussian fit to a A) full SASE spectrum, “pink beam” shot, and B) to a monochromatized shot, both from the February 2nd datasets. Gaussian center and FWHM are indicated in red. Intensity axes are log-scale.

Measurement data is summarized in Table 1. The RMS size of the X-ray pulse at the screen was found by taking the median of all 2D Gaussian RMS beam size fits. The size of the X-ray pulse at the source can be approximated by assuming Gaussian beam propagation from a waist at the source location, giving an estimated source size of  $\sim 40 \mu\text{m}$  in the November datasets, and  $\sim 20 \mu\text{m}$  for the February datasets. As indicated by the higher mean gas detector X-ray pulse energy, the FEL was more saturated in the February datasets, which may have reduced the X-ray pulse size at the source.

We examined whether X-ray pointing jitter correlated with the beamline variables we recorded. We found shots with high i0, and low amplitude (max-min) of the electron beam orbit, correlated strongly with reduced angular pointing jitter in both pink and monochromatized datasets. The November 13th monochromatized dataset is plotted in Fig. 4A-D, and the February 2nd pink beam dataset is shown in Fig. 4E-H. All four datasets showed low amplitude electron beam orbits correlated with reduced angular pointing jitter. The November 9th dataset where i0 represented the entire X-ray pulse energy rather than a monochromatic slice showed weak correlation between high i0 and reduced angular pointing jitter, but all three datasets where i0 represented the monochromatic X-ray pulse energy showed strong correlation between high i0 and reduced angular pointing jitter.

Figure 5 shows the pointing jitter in X and Y plotted in a 2D histogram for the November 13 monochromatized dataset. As seen in the plot, shots that have both high i0 and low electron beam orbit have the lowest pointing jitter.

Table 1: Measurement Summary

	11/9/20 Pink	11/13/20 Mono	2/2/21 Pink	2/2/21 Mono
# Undulators	26	26	32	32
X-ray Energy (keV)	9.002	9.863	9.981	9.981
$e^-$ Energy (GeV)	10.22	10.69	10.23	10.23
Source Distance (m)	134	134	159	135
RMS X-ray Size at Screen ( $\mu\text{m}$ )	150 X 160 Y	140 X 140 Y	330 X 360 Y	340 X 250 Y
Gas Detector (mJ)	0.86	0.76	1.4	1.4
Filtering Criteria: i0, orbit	>450 $\mu\text{J}^*$ , <10 $\mu\text{m}$	>12 $\mu\text{J}$ , <10 $\mu\text{m}$	>1 $\mu\text{J}$ , <10 $\mu\text{m}$	>1 $\mu\text{J}$ , <10 $\mu\text{m}$
Pointing Jitter, no filter (nrad)	367 X 279 Y	614 X 397 Y	629 X 266 Y	3365 X 992 Y
Pointing Jitter, filtered (nrad)	213 X 118 Y	286 X 229 Y	82 X 76 Y	288 X 202 Y
# Total Shots	23230	30649	2461	31026
# Filtered Shots	840	141	59	670

### Pointing Jitter for 7 Undulators

While the data shown thus far shows the pointing jitter of a saturated X-ray beam, for CBXFEL, we are interested in the pointing jitter of X-rays from seven undulator segments. However, since our screens are not sensitive enough to measure the radiation of seven undulators, we estimated this pointing jitter by measuring pointing jitter at 32, 27, 22 and 17 undulators, as shown in Fig. 6. This data was obtained on February 2nd, when 32 undulators were installed in HXU. To measure lasing at fewer than 32 undulators, a dipole kick was given by a corrector magnet after the appropriate number of undulators to prevent lasing in downstream undulators, and the source point was moved accordingly to calculate angular pointing. We then applied the same filtering discussed in the previous section to this dataset. In the filtered data shown in Fig. 6A & C, shots were filtered on electron beam orbit amplitude of less than 10  $\mu\text{m}$ , and i0 greater than 1, 1, 0.18, and 0.04 mJ for 32, 27, 22 and 17 undulators respectively. To account for the wide variation in pulse energy for a variable number of undulators, a variable i0 threshold was picked at the location where the slope leveled off in the pointing jitter versus i0 plot for the monochromatized beam.

We made a linear extrapolation using this data to estimate pointing jitter for seven undulators. Using the filtered data, we estimate approximately 150 nrad for the pink beam, and 400 nrad for the monochromatized beam. We note that these are order of magnitude estimates, as we have not studied pointing jitter far from FEL saturation, and a linear extrapolation may or may not be appropriate.

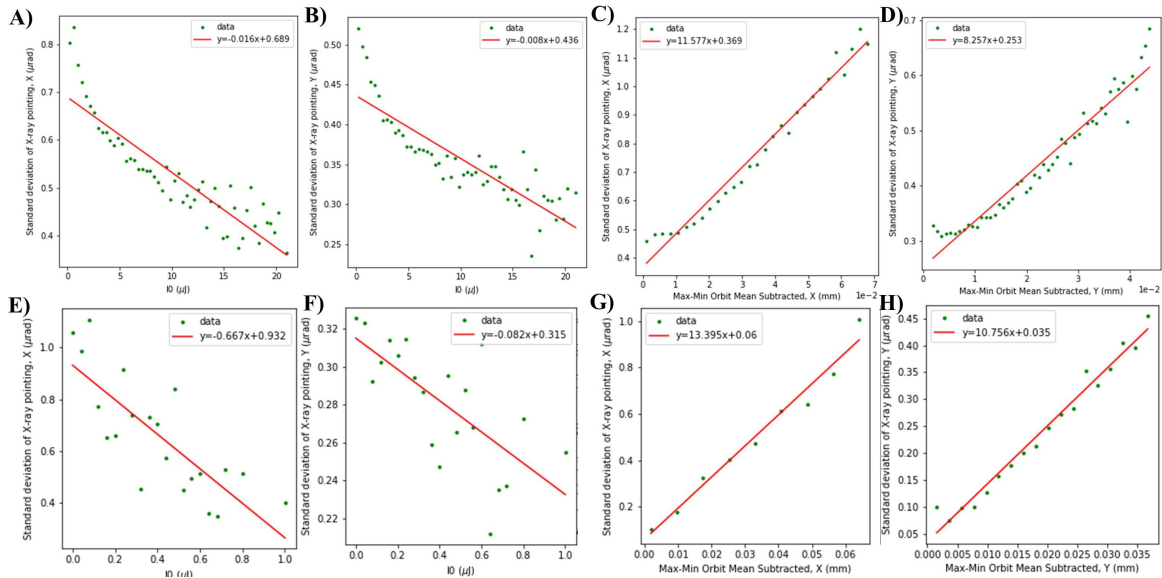


Figure 4: Standard deviation of X-ray pointing in X and Y binned with beamline variables (>30 shots/bin). A-D) show the November 13th monochromatized dataset. E-H) show the February 2nd pink beam dataset.

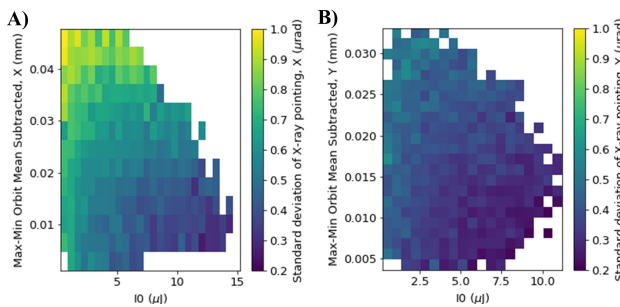


Figure 5: 2D histogram of pointing jitter for bins of  $i0$  and amplitude of the electron beam orbit for A) X and B) Y.

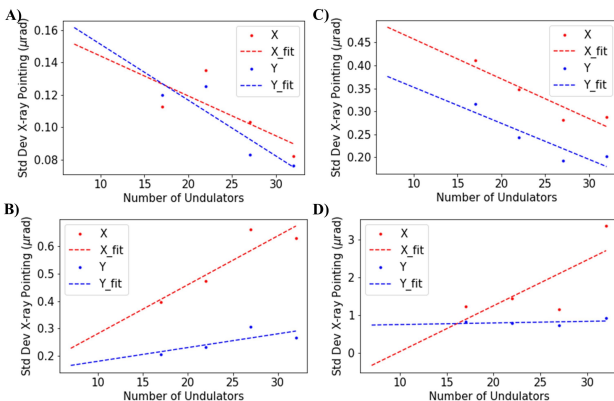


Figure 6: Estimate of pointing jitter for 7 undulators. Pointing jitter is plotted for a variable number of undulators for A-B) pink beam, and C-D) monochromatized beam. A&C show shots that have been filtered on  $i0$  and electron beam orbit amplitude, and B&D show all shots in the dataset.

## FUTURE DIRECTIONS

For future studies, we would like to measure pointing jitter with fewer numbers of undulators, and in conditions even

more closely mimicking CBXFEL. We could lase the last seven undulators at the end of HXU to test if our detectors are sensitive enough to measure the seven undulator radiation if the source point is closer. We could also measure the pointing jitter of X-rays reflected off one or more diamond (400) crystals. While the diamond (111) crystals in the XPP monochromator are oriented parallel to one another in a non-dispersive configuration, the CBXFEL crystals in our rectangular cavity will be oriented perpendicular to one another in a dispersive configuration. It would be interesting to study if there is a difference in the pointing jitter of beams which have passed through two crystals in a dispersive versus a non-dispersive series of reflections.

## CONCLUSION

We measured the pointing jitter for the full LCLS line, and estimated the pointing jitter for seven undulators. We identified that shots with high X-ray pulse energy of a monochromatic slice (" $i0$ "), and low amplitude of the electron beam orbit have reduced X-ray pointing jitter. The pointing jitter of the full LCLS line was larger for monochromatized beams than full SASE pink beam, and filtering on  $i0$  and electron beam amplitude reduced the pointing jitter by a factor of two or greater.

For CBXFEL, we can use these shot-to-shot  $i0$  and electron beam orbit filters to select shots with low pointing jitter to more accurately measure the FEL gain. We also note that since electron beam orbit amplitude has such a large impact on X-ray pointing jitter, that it will be worth spending time to flatten the electron beam orbit inside the CBXFEL cavity to reduce pointing jitter.

Content from this work may be used under the terms of the CC BY 3.0 licence (© 2021). Any distribution of this work must maintain attribution to the author(s), title of the work, publisher, and DOI

## REFERENCES

- [1] E. A. Schneidmiller and M. V. Yurkov, “Transverse coherence and pointing stability of the radiation from x-ray free electron lasers”, in *Proc. SPIE 10237*, Prague, Czech Republic, Jun. 2017, p. 102370I. doi:10.1117/12.2265567
- [2] G. Marcus *et al.*, “CBXFEL Physics Requirements Document for the Optical cavity Based X-Ray Free Electron Lasers Research and Development Project”, LCLS, CA, USA, Rep. SLAC-I-120-103-121-00, Apr 2020.
- [3] G. Marcus *et al.*, “Cavity-Based Free-Electron Laser Research and Development: A Joint Argonne National Laboratory and SLAC National Laboratory Collaboration”, in *Proc. FEL’19*, Hamburg, Germany, Aug. 2019, pp. 282–287. doi:10.18429/JACoW-FEL2019-TUD04
- [4] M. Chollet *et al.*, “The X-ray Pump-Probe instrument at the Linac Coherent Light Source”, *J. Synchrontron Rad.*, vol. 22, p. 503, 2015. doi:10.1107/S1600577515005135
- [5] D. Zhu *et al.*, “Performance of a beam-multiplexing diamond crystal monochromator at the Linac Coherent Light Source”, *Rev. Sci. Instrum.*, vol. 85, p. 063106, 2014. doi:10.1063/1.4880724